

See discussions, stats, and author profiles for this publication at: <https://www.researchgate.net/publication/10783484>

# Size-Selective Organization of Enthalpic Compatibilized Nanocrystals in Ternary Block Copolymer/Particle Mixtures

ARTICLE *in* JOURNAL OF THE AMERICAN CHEMICAL SOCIETY · JUNE 2003

Impact Factor: 12.11 · DOI: 10.1021/ja034523t · Source: PubMed

CITATIONS

310

READS

89

## 4 AUTHORS, INCLUDING:



**Michael R Bockstaller**

Carnegie Mellon University

92 PUBLICATIONS 2,249 CITATIONS

SEE PROFILE



**Yonit Boguslavsky**

Agricultural Research Organization ARO

7 PUBLICATIONS 427 CITATIONS

SEE PROFILE



**Edwin L Thomas**

Rice University

618 PUBLICATIONS 23,976 CITATIONS

SEE PROFILE

## Size-Selective Organization of Enthalpic Compatibilized Nanocrystals in Ternary Block Copolymer/Particle Mixtures

Michael R. Bockstaller,<sup>†</sup> Yonit Lapetnikov,<sup>‡</sup> Shlomo Margel,<sup>‡</sup> and Edwin L. Thomas<sup>\*,†</sup>*Department of Materials Science and Engineering, Massachusetts Institute of Technology, 77 Massachusetts Avenue, Cambridge, Massachusetts 02139, and Department of Chemistry, Bar-Ilan University, Ramat Gan 52900, Israel*

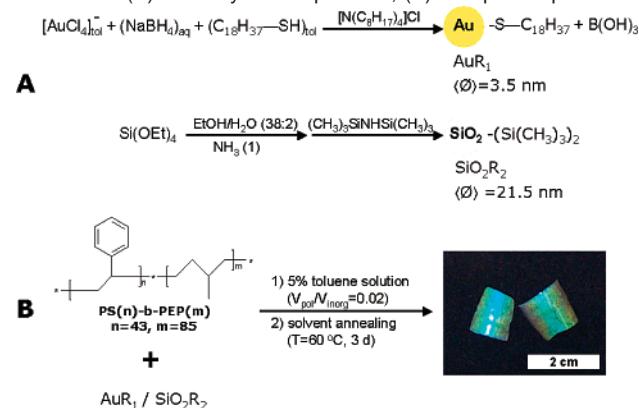
Received February 5, 2003; E-mail: elt@mit.edu

The effective control of the spatial organization and connectivity of nanosized matter is an important prerequisite for the technological utilization of nanocrystal research. The ability to control both the length scale and the spatial organization of block copolymer morphologies makes these materials particularly attractive as scaffolds for engineering of nanostructures and has motivated a variety of studies, for example, the kinetically driven patterning of polymer surfaces by preferential wetting with evaporated metals or nanoreactor schemes in which nanocrystals are synthesized within block copolymer scaffolds that have been loaded with a suitable precursor reagent.<sup>1</sup> The simultaneous self-organization of block copolymers in the presence of ex-situ synthesized particles provides yet another approach to engineer 2D and 3D nanostructures that facilitates better control of the structural characteristics of the sequestered component, which becomes important when applications rely on size- or shape-related properties of nano-objects.<sup>2</sup>

In this contribution, we demonstrate the hierarchical pattern formation of binary mixtures of nanocrystals and high-molecular weight block copolymers by strategic design of the nanocrystals. We identify two distinct types of particle-morphology dependent on the particle-core size, that is, the localization of particles along the intermaterial dividing surface (IMDS) or at the center of the respective polymer domain. Even more interesting, in ternary systems consisting of block copolymer and two different-sized nanocrystal species, the distinct morphological types are conserved, resulting in autonomous separation and organization of the respective nanocrystals within alternating arrays and sheets.

The system in our study consists of a symmetric poly(styrene-*b*-ethylene propylene) (PS-PEP) copolymer with a molecular weight of the respective blocks of  $4 \times 10^5$  g/mol as well as aliphatic-coated gold and silica nanocrystals. The lamellar morphology of the block copolymer with domain spacings of 100 nm for the PS and 80 nm for the PEP domain was confirmed by ultra-small-angle X-ray scattering.<sup>2</sup> The gold nanocrystals were synthesized using a phase-transfer procedure as described by Brust et al.<sup>3</sup> Monodispersed silica nanoparticles of narrow size distribution were prepared by polymerization of tetraethyl orthosilicate, according to a modification of the Stober's method by adding tetraethyl orthosilicate (0.6 mmol) to ethanol (38 mmol) solution containing superpure water (2.4 mmol) and ammonia (30%, 1 mol).<sup>4</sup> The solution was stirred for 7 days, and hexamethylenedisilazane was added (final concentration 1.5 M). After being stirred for 2 days, the nanocrystals were extracted in 10 mL of toluene. Both synthetic procedures are outlined in Scheme 1.

Particle characterization was performed using a JEOL 2000FX transmission electron microscope (TEM) and confirmed by UV/vis absorption spectroscopy (using a Cary 5E UV-vis-NIR dual-

**Scheme 1.** (A) Nanocrystal Preparation, (B) Sample Preparation<sup>a</sup>

<sup>a</sup> The photograph shown in (B) represents the Au-nanocrystal sample. The greenish colors arise due to Bragg-reflectance from the multilayered polymer domains.

beam spectrophotometer) as well as photon correlation spectroscopy (using a Brookhaven 9000 AT dynamic light-scattering apparatus) in the case of the silica nanocrystals. Image analysis of electron micrographs of the respective nanocrystals after casting the particle suspension onto carbon film revealed a particle diameter of  $d_{\text{core}} = 3.5 \pm 1$  nm in the case of the gold and  $d_{\text{core}} = 21.5 \pm 2.5$  nm for the silica nanocrystals.<sup>5</sup> A comparable grafting density for both types of nanoparticles, that is, densities of  $\rho_{\text{Au}} \approx 0.22$  S-atoms/ $\text{\AA}^2$  and  $\rho_{\text{SiO}_2} \approx 0.59$  C-atoms/ $\text{\AA}^2$ , was determined by elemental analysis. The block copolymer/nanocrystal composite films were subsequently obtained by casting a 5% polymer solution in toluene admixed with nanocrystals to result in a final amount of inorganic component in the composite of 2 vol %. Films of about 1 mm in thickness were obtained and annealed in saturated solvent atmosphere for 96 h at  $60^\circ\text{C}$  to obtain near equilibrium conditions before drying in a vacuum for 48 h.<sup>6</sup> The resulting films were microsectioned at  $-90^\circ\text{C}$  using a Reichert–Jung ULTRACUT microtome and imaged without further staining using amplitude and phase contrast. Electron micrographs obtained after sectioning the film normal to the layer direction as shown in Figure 1 reveal two distinct types of particle arrangement for the respective nanocrystals within the composite.

Gold nanocrystals are found to segregate to the IMDS between the PS and PEP domains, whereas the larger silica nanocrystals are mostly located at the center of the PEP domains. As both nanocrystals are aliphatic coated, enthalpic compatibilization is expected to yield a bias driving the particles within the PEP domains. Neglecting any difference in enthalpic interactions between the two types of nanocrystals and the polymer matrix, our results suggest a profound influence of entropic contributions to the self-organization process. This interpretation is substantiated

<sup>†</sup> Massachusetts Institute of Technology.<sup>‡</sup> Bar-Ilan University.

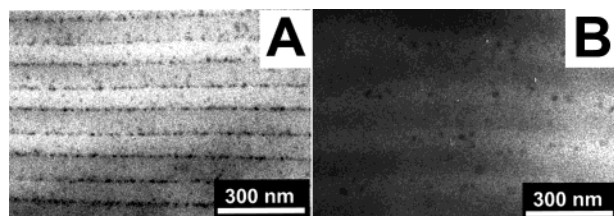


**Figure 1.** Bright field electron micrographs of binary blends (A) PS-PEP + AuR<sub>1</sub> and (B) PS-PEP + SiO<sub>2</sub>R<sub>2</sub> with inorganic filling fraction  $\phi = 0.02$ , demonstrating particle deposition at (A) IMDS and (B) center of PEP domain. PEP-domains appear as brighter regions in the micrograph (no stain). In both cases, the cutting direction of the films was normal to the layer direction.

by recent theoretical studies that predict the formation of ordered mesophases in block copolymer/particle composites due to entropically driven particle segregation.<sup>7</sup> Using a mean field approach, it was shown for a 2D system representing a mixture of nanoparticles within a lamellar block copolymer in the intermediate segregation limit that interfacial segregation of particles is expected to occur for particle sizes  $d/L < 0.2$ , whereas concentration of the particles at the center of the domain is expected for  $d/L > 0.3$ , where  $d$  is the particle, and  $L$  is the respective domain dimension. Even though our system represents the case of strong segregation and the simulation does not account for the effect of surface grafted groups, our results follow the theoretical prediction as we find  $d/L \approx 0.06$  for the gold particles and  $d/L = 0.26$  for the silica particles.<sup>8</sup> The agreement between the simulated and experimentally observed morphologies suggests that the structure formation process is determined by predominantly entropic contributions. For large particles, the decrease in conformational entropy of the respective polymer subchains upon particle sequestration is dominant, whereas for smaller particles, the decrease in entropy is outweighed by the particle's translational entropy.<sup>7,9</sup> We note that this interpretation is preliminary and more exhaustive studies about the effect of ligand chemistry on enthalpic compatibilization and particle interaction within the composite are underway.

Interestingly, as revealed in Figure 2, the morphological characteristics of the two different binary particle/block copolymer mixtures are retained in the ternary particle1/particle2/block copolymer mixture and result in autonomous particle separation and organization into a stacklike structure comprising alternating sheets of silica and gold nanocrystals. No misplacements in the particular particle locations could be observed over areas of  $4 \mu\text{m}^2$ , indicating a strong thermodynamic driving force toward the individual structural states.

Our results demonstrate that self-assembly of block copolymers and strategically designed nanocrystals provides a route toward hierarchically ordered multicomponent materials in which the 3D connectivity is implied by the morphology of the template block copolymer and the location of nanoscopic insertions is determined by the characteristic length scales of the materials. This provides new perspectives to engineer high-performance composite materials in which the inserted particles are located in regions that allow efficient capitalization of their characteristic properties.

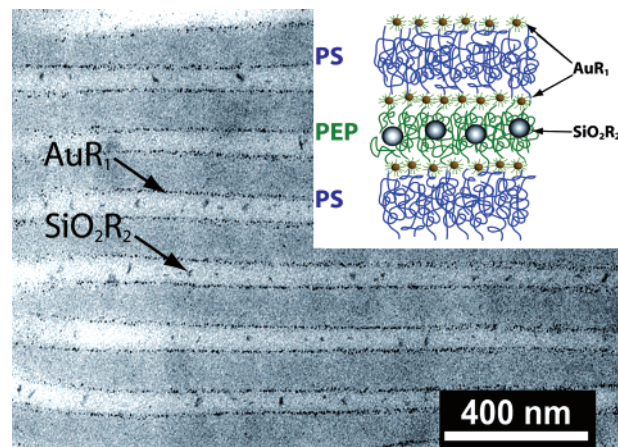


**Figure 2.** Bright field electron micrograph of a ternary blend of PS-PEP + AuR<sub>1</sub> + SiO<sub>2</sub>R<sub>2</sub> with inorganic filling fraction  $\phi = 0.02$ , respectively, after microsectioning normal to the layer direction (no stain). Gold nanocrystals appear as dark spots along the IMDS; silica nanocrystals reside in the center of the PEP domain. Inset: Schematic of the particle distribution (size proportions are changed for clarity).

Furthermore, the naturally occurring size-selective organization of the nanocrystals presents opportunities for the regular patterning of surfaces with multiple different-sized nanocrystal species with complementary chemical or physical characteristics on sub-100 nm length scales.

**Acknowledgment.** This material is based upon work supported by the U.S. Army Research Laboratory and the U. S. Army Research Office under Contract DAAD-19-02-0002, the Israel-United States Binational Foundation, and the Alexander von Humboldt Foundation (Feodor-Lynen Program).

**Supporting Information Available:** Electron micrographs and size distribution of nanocrystals (PDF). This material is available free of charge via the Internet at <http://pubs.acs.org>.

## References

- (1) Lopes, W. A.; Jaeger, M. J. *Nature* **2001**, *414*, 735–738. Morkoved, T. L.; Wiltzius, P.; Jaeger, H. M.; Grier, D. G.; Witten, T. A. *Appl. Phys. Lett.* **1994**, *64*, 422–424. Boontongkong, Y.; Cohen, R. E. *Macromolecules* **2002**, *35*, 3647–3652. Joly, S.; Kane, R.; Radzilowski, L.; Wang, T.; Wu, A.; Cohen, R. E.; Thomas, E. L.; Rubner, M. L. *Langmuir* **2000**, *16*, 1354–1359. Tadd, E. H.; Bradley, J.; Tannenbaum, R. *Langmuir* **2002**, *18*, 2378–2384.
- (2) Hamdoun, B.; Ausserre, D.; Gabuil, V.; Gallot, Y.; Clinard, C.; Joly, S. *J. Phys. II* **1996**, *4*, 493–501. Bockstaller, M. R.; Kolb, R.; Thomas, E. L. *Adv. Mater.* **2001**, *13*, 1783–1786.
- (3) Brust, M.; Walker, M.; Bethell, D.; Schiffrin, D. J.; Whyman, R. *J. Chem. Soc., Chem. Commun.* **1994**, 801–803.
- (4) Stober, W.; Fink, A.; Bohn, E. *J. Colloid Interface Sci.* **1968**, *26*, 62–65. Brandriss, S.; Margel, S. *Langmuir* **1993**, *9*, 1232–1240.
- (5) See Supporting Information.
- (6) One reference sample that was annealed for 14 days was used to confirm near equilibrium conditions.
- (7) Thompson, R. B.; Ginzburg, V. V.; Matsen, M. W.; Balazs, A. C. *Science* **2001**, *292*, 2469–2472. Huh, J.; Ginzburg, V. V.; Balazs, A. C. *Macromolecules* **2000**, *33*, 8085.
- (8)  $d = d(\text{core}) + d(\text{corona})$ , with  $d(\text{corona}) = 1.5 \text{ nm}$  ( $\text{SC}_{18}\text{H}_{37}$ ),  $0.7 \text{ nm}$  ( $\text{Si}(\text{CH}_3)_2$ ).
- (9) Lee, J.-Y.; Thompson, R. B.; Jasnow, D.; Balazs, A. C. *Phys. Rev. Lett.* **2002**, *89*, 155503, 1–4. Kim, J. U.; O'Shaughnessy, B. *Phys. Rev. Lett.* **2002**, *89*, 238301, 1–4.

JA034523T